AIAA 80-0716R

Scale-Free Refined Element Technique

John O. Dow*
University of Colorado, Boulder, Colo.
and
Doyle E. Byrd†
Duke Power Company, Charlotte, N.C.

Scale-free finite elements are elements whose stiffness properties depend only on relative dimensions and material constants. These elements are used in conjunction with standard finite-element techniques to formulate refined elements that are applicable to problems of different dimensions. This generalization of the refined-element method is illustrated with the case of a square shear panel containing a circular hole. Eigenvalue techniques are employed to show that the stiffness properties of this refined element are improved when it is modeled with a larger number of elements while retaining the same number of edge nodes. The accuracy of the resulting stress concentration factor remains essentially constant as the hole is located at different positions in a stress field.

Nomenclature

E = Young's modulus of elasticity
t = uniform thickness
v = Poisson's ratio
x,y = element coordinate system
x_i,y_i = nodal location of the ith node
α = ratio of lengths (a/b for a rectangle, $(x_2-x_3)/x_2$ for a triangle)
β = ratio of lengths ($(x_2-x_3)/y_3$ for a triangle)

Introduction

THE finite element method is used extensively to investigate stress concentrations in structures. The two most common finite element approaches have their shortcomings when high stress gradients are expected. On the one hand, if a large number of elements is used to model a stress concentration, the size of the problem can become unmanageable and numerical difficulties have been reported due to the large differences in the magnitudes of the stiffness coefficients.[1] On the other hand, the coarse-to-fine mesh technique, while not introducing a large number of coordinates, does not necessarily model the stress gradient or the effect of the stress concentration on the overall problem very well.

The developments presented provide a means of accurately modeling stress concentrations without introducing a large number of additional coordinates or any numerical difficulties by generalizing the refined element method. This generalization is accomplished through the use of scale-free and dimensionless finite elements in conjunction with standard finite-element assembly and static condensation techniques. The existence of these elements is well known,[2] but they have not been extensively studied or exploited until now.

Presented as Paper 80-0716 at the AIAA/ASME/ASCE/AHS 21st Structures, Structural Dynamics and Materials Conference, Seattle, Washington, May 12-14, 1980; submitted June 9, 1980; revision received Feb. 9, 1981.

*Assistant Professor, Department of Civil, Environmental and Architectural Engineering.
†Engineer, Design Engineering Department.

A scale-free element is a finite element for which the individual stiffness terms depend only on ratios of element dimensions and on the material properties. Thus, the stiffness matrix for two different-sized elements of the same shape and orientation are identical. General rectangular and triangular scale-free finite elements are used in this presentation.

Dimensionless finite elements are special cases of scale-free elements and the stiffness matrix depends solely on the material properties. Dimensionless finite elements result when a specific geometry is used in a general scale-free element. When these elements are applied to a larger, more complex problem, the resulting stiffness matrix is also dimensionless. Thus, the stiffness matrix developed for a specific stress concentration problem is the same regardless of the size of the problem and, hence, can be applied without change to other problems with different dimensions.

The example of a square shear panel containing an internal circular hole is studied in detail. It is shown that the stiffness properties of this refined element are improved when it is modeled with a larger number of elements while retaining the same number of edge nodes. It is also found that the accuracy of the stress concentration factors of specific location remains essentially constant as the hole is positioned at different locations in a stress field. The stiffness matrix is applicable regardless of the hole size; for example, the same stiffness matrix may be used whether the hole is 2 in. or 3 ft in diameter. If the panel thickness is changed, the stiffness matrix is modified by a simple scalar multiplication of each element of the stiffness matrix by the ratio of the new thickness to the old thickness. The actual stress value is determined by auxiliary calculations and is inversely proportional to the dimensions of the problem. The general conclusion is that highly refined, accurate stress concentration elements developed with a one-time effort can be used in larger structures without introducing a great number of coordinates or numerical difficulties into the overall stiffness matrix and can be reused in problems of different physical dimensions.

Scale-Free and Dimensionless Finite Elements

The coordinates for a scale-free rectangular isoparametric element are shown in Fig. 1a. The stiffness matrix that results when the assumed displacement field is a two-dimensional

application of Lagrange's interpolation formula is

$$\frac{Dt}{12}\begin{vmatrix}
K_1 & & & & & & & \\
K_2 & K_6 & & & & & & \\
K_3 & -K_4 & K_1 & & & SYM & & \\
K_4 & K_7 & -K_2 & K_6 & & & & \\
-\frac{K_1}{2} & -K_2 & K_5 & -K_4 & K_1 & & & \\
-K_2 & -\frac{K_6}{2} & K_4 & K_8 & K_2 & K_6 & & \\
K_5 & K_4 & -\frac{K_1}{2} & K_2 & K_3 & -K_4 & K_1 & \\
-K_4 & K_8 & K_2 & \frac{K_6}{2} & K_4 & K_7 & -K_2 & K_6
\end{vmatrix}$$

where

$$K_1=4(1/\alpha+\alpha D_{33}) \qquad K_5=4(\tfrac{1}{2}\alpha-\alpha D_{33})$$

$$K_2=3(D_{12}+D_{33}) \qquad K_6=4(\alpha+D_{33}/\alpha)$$

$$K_3=4(-1/\alpha+\alpha D_{33}/2) \qquad K_7=4(\alpha/2-D_{33}/\alpha)$$

$$K_4=3(D_{12}-D_{33}) \qquad K_8=4(-\alpha+D_{33}/2\alpha)$$

and for

Plane stress	Plane strain
$D=\frac{E}{(1-v^2)}$	$D=\frac{E(1-v)}{(1+v)(1-v)}$
$D_{12}=v$	$D_{12}=\frac{v}{(1-v)}$
$D_{33}=\frac{(1-v)}{2}$	$D_{33}=\frac{(1-2v)}{2(1-v)}$

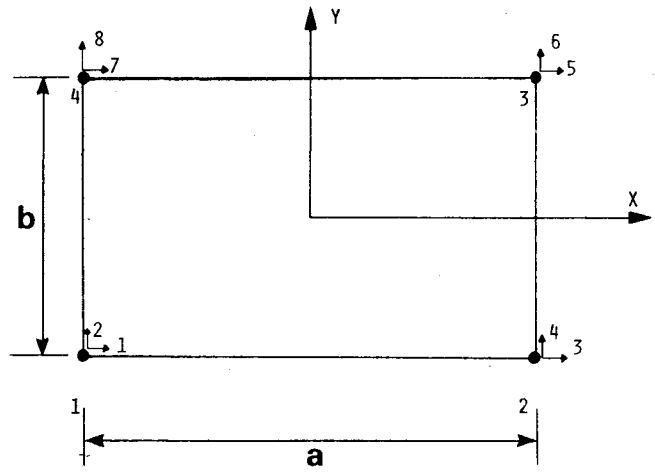

a)

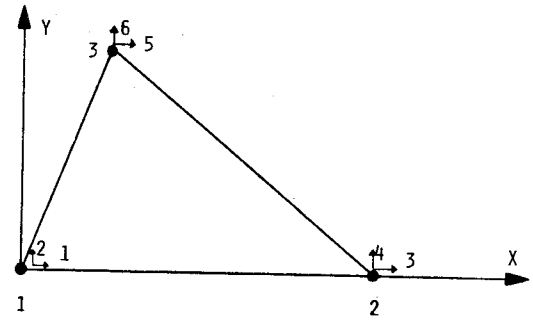

b)

Fig. 1 Coordinate systems for a scale-free rectangular and a triangular finite element.

The stiffness matrix contains only eight unique elements and each of these elements depends only on the ratio of the lengths of the sides of the rectangle and the material properties. Thus, the stiffness matrix does not depend on the absolute size of the rectangle being represented. When this stiffness matrix is evaluated as a plane stress square with unit thickness and the material properties of steel, the result is

$$10^7\begin{vmatrix}
1.484 & & & & & & & \\
0.536 & 1.484 & & & & & & \\
-0.907 & 0.041 & 1.484 & & & & & \\
-0.041 & 0.165 & -0.536 & 1.484 & & & & \\
-0.742 & -0.536 & 0.165 & 0.041 & 1.484 & & & \\
-0.536 & -0.742 & -0.041 & -0.901 & 0.536 & 1.484 & & \\
0.165 & -0.041 & -0.742 & 0.536 & -0.907 & 0.041 & 1.484 & \\
0.041 & -0.907 & 0.536 & -0.742 & -0.041 & 0.165 & -0.536 & 1.484
\end{vmatrix}$$

This dimensionless stiffness matrix is applicable to a steel square of any size and the thickness can be changed by a simple scalar multiplication.

The coordinates for a scale-free general triangular element are presented in Fig. 1b. The stiffness matrix of this constant strain triangle is

$$\frac{Dt}{2}\begin{vmatrix}
\frac{\alpha}{\beta}+D_{33}\alpha\beta & & & & \\
\alpha(D_{12}+D_{33}) & \alpha\beta+\frac{D_{33}\alpha}{\beta} & & & \\
-\frac{\alpha}{\beta}+D_{33}(1-\alpha) & D_{33}(1-\alpha)-\alpha D_{12} & \frac{\alpha}{\beta}\frac{D_{33}\beta}{\alpha}(1-\alpha)^2 & SYM & \\
D_{12}(1-\alpha)-\alpha D_{33} & -\frac{D_{33}\alpha}{\beta}+\beta(1-\alpha) & -(D_{12}+D_{33})(1-\alpha) & \frac{D_{33}\alpha}{\beta}+\frac{\beta}{\alpha}(1-\alpha)^2 & \\
-\beta D_{33} & -D_{33} & D_{33}\left(\beta-\frac{\beta}{\alpha}\right) & D_{33} & \frac{D_{33}\beta}{\alpha} \\
-D_{12} & -\beta & D_{12} & D_{12}\left(\beta-\frac{\beta}{\alpha}\right) & 0 \quad \frac{\beta}{\alpha}
\end{vmatrix}$$

The elements of this matrix depend only on the ratio of specific dimensions of the triangle and the material properties. The stiffness matrix is scaled for thickness by a simple scalar multiplication. Thus, the stiffness elements depend on the shape of the triangle and not on the absolute size of the triangle.

Composite Elements

Refined composite square and quadrilateral elements assembled from scale-free and dimensionless elements are analyzed singly and in simple structures to determine convergence and stiffness properties of the resulting dimensionless finite elements. The first element considered is the composite square composed of four square dimensionless elements as shown in Fig. 2a. The edge nodes are eliminated using a linear interpolation transformation which retains interelement compatibility and the coordinates of the inner node are eliminated using static condensation techniques. The result is a square element with eight degrees of freedom as shown in Fig. 2c. This new eight-degree-of-freedom square is then used to create another composite square, which is, in turn, reduced to a square containing eight explicit degrees of freedom. When continued, this recursive procedure results in a dimensionless square implicitly containing many more degrees of freedom than are introduced into a problem.

The stiffness matrix of each successive composite square retains the structure of the stiffness matrix of the original square element. That is to say, the stiffness matrix contains only eight unique elements and they are arranged in the same pattern as in the original stiffness matrix. These eight unique matrix elements converged as follows. Matrix elements of the type K_{12}, K_{14}, K_{16}, and K_{18} remained the same after each iteration. Matrix elements of the K_{11}, K_{13}, K_{15}, and K_{17} type followed an asymptotic convergence pattern. Each matrix element approached an asymptote after three or four iterations. The lack of a more rapid convergence pattern indicates that the stiffness properties of the element are heavily influenced by the straight-line constraint on the edge of the element. A similar analysis of a composite square composed of nine square dimensionless elements, as shown in Fig. 2b, resulted in a similar convergence pattern for the eight unique elements of the stiffness matrix. The same asymptote was approached in fewer iteration steps for the converging matrix elements when nine subelements were used instead of four.

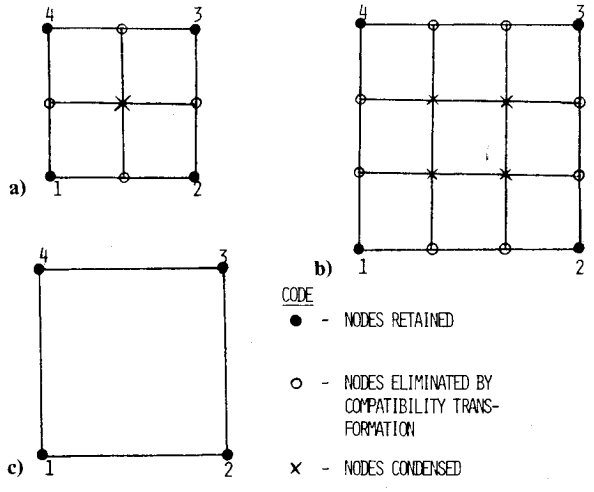

Fig. 2 Composite elements: a) four subsquare composite element; b) nine subsquare composite element; c) dimensionless square element after nodal elimination.

By this process, generally applicable refined finite elements are formed using numerical calculations instead of analytic manipulations using symbols. In addition, this analysis shows that the inclusion of a large number of elements in a composite element does not substantially increase the differences between the magnitudes of the numbers contained in the stiffness matrix. This implies that the use of large numbers of these elements in a specific problem will produce no unforeseen numerical difficulties during the solution process.

The overall stiffness properties of the composite elements cannot be directly compared by studying the convergence patterns of the individual elements of the stiffness matrix. The stiffness properties are compared through the use of the eigenvalues and the eigenvectors of the composite elements. The eigenvalue calculation is equivalent to subjecting the element to a loading condition with the load proportional to the nodal displacements. The resulting eigenvectors represent a set of linearly independent deflection modes. The eigenvalues are proportional to the stiffness of the respective independent modes of displacement. Thus, a similar element with smaller eigenvalues is the softer element and, hence, the better model since a compatible finite element formed using an assumed displacement field is stiffer than the continuum it represents.[1]

The eight linearly independent displacement modes in increasing order of eigenvalues are shown in Fig. 3 for the original eight-degrees-of-freedom dimensionless square. The first three modes are rigid body displacements with eigenvalues equal to zero. This matches the kinematically required number of rigid body modes for a planar problem. The first two flexible modes are linear strain modes corresponding to flexural deformations. The eigenvalues are equal for these mirror-image modes. The next three flexible modes are constant strain modes. The first of these modes represents pure shear deformation, the second is a pinching deformation, and the last mode is a uniform extension deflection.

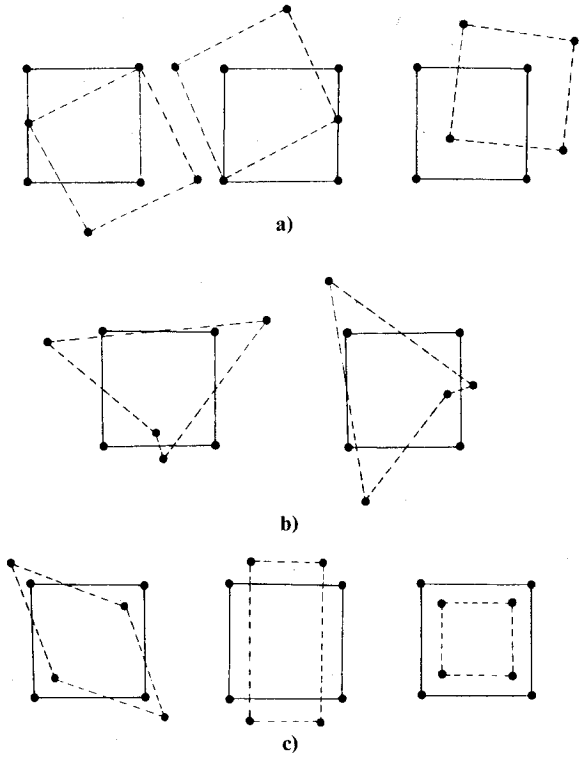

Fig. 3 Mode shapes for dimensionless square finite element: a) rigid body mode shapes; b) linear strain (flexure) mode shapes; c) constant strain mode shapes.

Table 1 Eigenvalues for four subsquare composite elements—flexible modes only

Strain type	Eigenvalues for iteration no. (1.0×10^8)				
	Basic	1	2	3	4
Linear	0.17308	0.14303	0.13415	0.13151	0.13072
Linear	0.17308	0.14303	0.13415	0.13151	0.13272
Constant	0.23077	0.23077	0.23077	0.23077	0.23077
Constant	0.23077	0.23077	0.23077	0.23077	0.23077
Constant	0.57692	0.57692	0.57692	0.57692	0.57692
Sum	1.38462	1.32452	1.30677	1.30148	1.29990

Table 2 Eigenvalues for nine subsquare composite elements—flexible modes only

Strain type	Eigenvalues for iteration no. (1.0×10^8)				
	Basic	1	2	3	4
Linear	0.17308	0.13450	0.12924	0.12851	0.12841
Linear	0.17308	0.13450	0.12924	0.12851	0.12851
Constant	0.23077	0.23077	0.23077	0.23077	0.23077
Constant	0.23077	0.23077	0.23077	0.23077	0.23077
Constant	0.57692	0.57692	0.57692	0.57692	0.57692
Sum	1.38462	1.30745	1.29693	1.29549	1.29529

The five nonzero eigenvalues for the original square and four successive four-element composite squares are given in Table 1. The same information for the nine-element composite square is provided in Table 2. In both cases, the sum of the eigenvalues for each successively developed dimensionless square is sequentially smaller and the sums of the eigenvalues of the nine-element composites are smaller than the sums for the four-element composites at each iteration. This indicates that each successive composite element is a better overall model than the previous element for both cases and that the nine-element composite is a better model than the four-element composite. All of the reduction in the sums of the

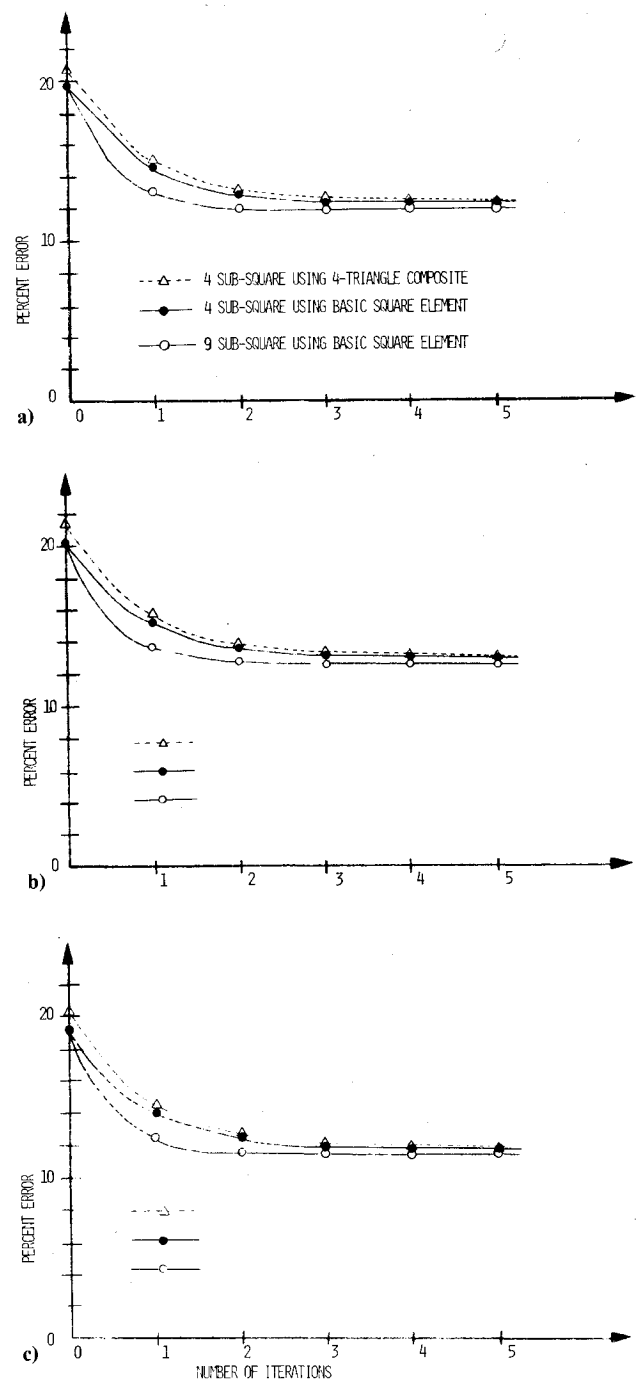

Fig. 4 Cantilever tip deflection error: a) end shear loading; b) end moment loading; c) uniform loading.

eigenvalues is a reduction in the eigenvalues corresponding to the flexure modes (modes 4 and 5). These eigenvalues converge to an asymptote and the largest change occurs in the first iteration step. The eigenvalues of the constant strain modes remain the same. This can be interpreted to mean that the modeling of the flexural deflections is improved by adding the implicit internal degrees of freedom while the modeling of the constant strain modes is not improved. Thus, the flexural stiffness properties of these recursive elements are improved when a larger number of elements are included inside of the element while retaining the same number of edge nodes.

This improvement in the flexural characteristics of the composite element is further illustrated when the tip deflections of a loaded slender cantilever beam modeled with these elements are compared to the Euler-Bernoulli solution. A cantilever beam with an aspect ratio of 10:1 is modeled

using a 2×20 array of square elements and is loaded with an end shear, an end moment, and a uniformly distributed load. The improvement in the tip deflection as a function of the degree of refinement of the dimensionless square element is shown for each loading condition in Figs. 4a-c. The tip deflection converges to an asymptote and the largest improvement occurs in the first refinement. Also, the nine-element composite gives slightly better results than the four-element composite at each iteration step. The error in the fiber stress at the center of an element for the end-moment loading is shown in Fig. 5. Again, the results reach an asymptote with the first step showing the greatest improvement and the nine-element composite giving the better results. The shear stresses are the same for the various composite elements for these loading conditions. The convergence pattern for these stresses follow the pattern of convergence shown by the eigenvalues of the composite elements for both flexure and shear.

A similar analysis of loaded cantilever beams is performed using a different dimensionless square element as the starting point for creating four-element composites. The new dimensionless square element is composed of four constant strain triangles with the internal degrees of freedom eliminated as shown in Fig. 6a. The tip deflections of the three loading conditions are shown in Figs. 4a-c. The results for this element converge to the same values as for the other four-element composite, with the new element being slightly stiffer at each iteration step.

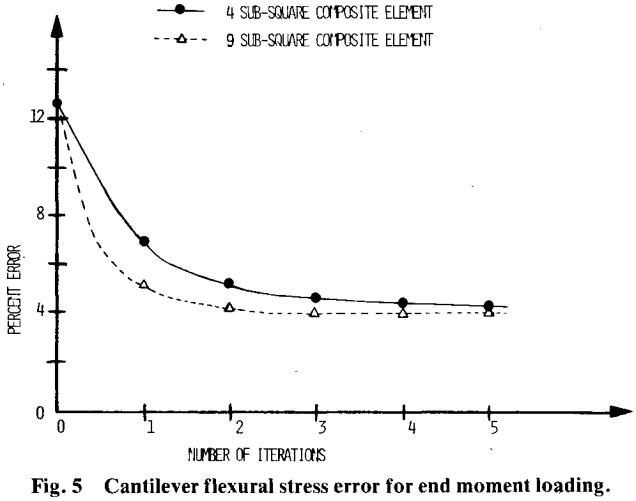

Fig. 5 Cantilever flexural stress error for end moment loading.

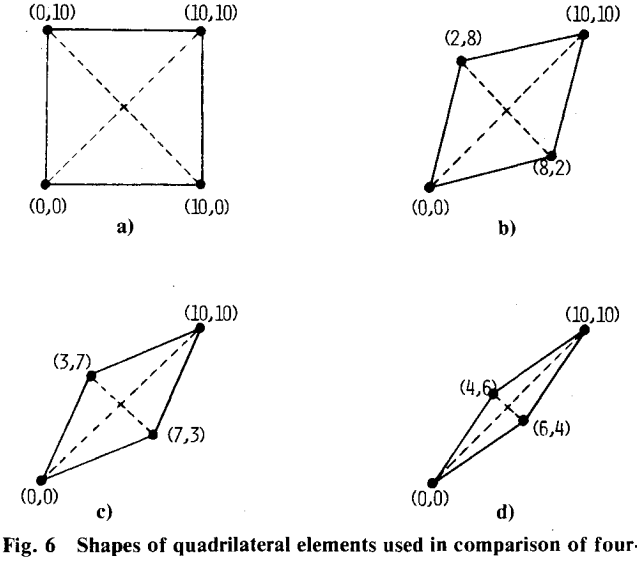

Fig. 6 Shapes of quadrilateral elements used in comparison of four-triangle composite and isoparametric elements.

In addition to the analysis of the stiffness properties of a composite square element composed of four constant strain triangles, the stiffness properties of distorted quadrilateral elements composed of four constant strain triangles are compared to the stiffness properties of identically shaped isoparametric quadrilateral elements. The shapes analyzed are shown in Fig. 6. The stiffening of isoparametric elements when they are distorted is well known.[3-7]

The eigenvalues and eigenvectors for the composite and isoparametric elements shown in Fig. 6 are calculated as a measure of their stiffness properties. The eigenvectors for both types of elements for each shape are identical and have shapes similar to those shown in Fig. 3. The five nonzero eigenvalues for the square element (Fig. 6a) are given in Table 3. The eigenvalues for the three constant strain modes of deflection are given first and are identical for the composite-square element and for the square isoparametric element. The eigenvalues for the flexural modes are slightly stiffer in the case of the composite square. Thus, the square isoparametric element models the flexural modes of deflection slightly better than the square composite element by 3.6%. This same conclusion is reached by comparing the cantilever beam tip deflections for the basic elements shown in Figs. 4a-c.

The five nonzero eigenvalues for the distorted elements shown in Figs. 6b-d are given in Tables 4-6, respectively. In all three cases, the eigenvalues for the constant strain modes are the same for the composite element as for the isoparametric element. The flexural modes for all three distorted shapes are softer for the composite element than for the isoparametric element. The flexural modes are softer by 13.3% for element b, by 41.2% for element c, and by 79.2% for element d. Thus,

Table 3 Eigenvalues for isoparametric and composite elements for a distorted element shown in Fig. 6a

Strain type	Eigenvalues by type (10^8)	
	Isoparametric	Composite
Constant	0.23077	0.23077
Constant	0.23077	0.23077
Constant	0.57693	0.57693
Linear	0.17308	0.17949
Linear	0.17308	0.17949
Sum	1.38462	1.39742

Table 4 Eigenvalues for isoparametric and composite element for distorted element shown in Fig. 6b

Strain type	Eigenvalue by type (10^8)	
	Isoparametric	Composite
Constant	0.13138	0.18138
Constant	0.26154	0.26154
Constant	0.73399	0.73399
Linear	0.14487	0.12555
Linear	0.24743	0.21443
Sum	1.56921	1.51689

Table 5 Eigenvalues for isoparametric and composite elements for distorted element shown in Fig. 6c

Strain type	Eigenvalues by type (10^8)	
	Isoparametric	Composite
Constant	0.12757	0.12757
Constant	0.33462	0.33462
Constant	1.04356	1.04356
Linear	0.15000	0.08827
Linear	0.35192	0.20710
Sum	2.00767	1.80112

Table 6 Eigenvalues for isoparametric and composite elements for distorted element shown in Fig. 6d

Strain type	Eigenvalues by type (10^8) Isoparametric	Composite
Constant	0.06543	0.06543
Constant	0.60000	0.60000
Constant	2.03453	2.03453
Linear	0.21923	0.04563
Linear	0.68076	0.14170
Sum	3.59996	2.88730

ELEMENT CONFIGURATION (P=100, E=10x10^6, ν=0.3)	TIP DEFLECTION (10^{-4}) ISOPARAMETRIC	COMPOSITE
0,10 100,10 P 0,0 100,0	1.0	0.7
50,10 P 50,0	3.8	2.7
25,10 75,10 P 25,0 75,0	11.5	8.8
75,10 P 25,0	1.5	1.9
83.33,10 P 16.67,0	2.2	3.4
15,10 85,10 P 45,0 55,0	2.4	2.9

Fig. 7 Tip deflection of a cantilever beam (unit thickness) by isoparametric and composite elements.

the composite elements model the flexural modes in the distorted elements progressively better than the isoparametric elements as the distortion increases.

This comparison of the flexural characteristics of distorted composite and isoparametric elements is further illustrated when the tip deflections resulting from an end load on a slender cantilever are compared. The tip deflection and the element configuration for a cantilever beam with an aspect ratio of 10:1 are shown in Fig. 7. The isoparametric elements are softer than the composite elements for the rectangular cases. The composite elements are softer than the isoparametric elements for the distorted cases. This result is consistent with the results of the eigenvalue analysis. Stricklin et al.[8] have compared various higher-order quadrilateral isoparametric and composite linear strain triangular elements (eight-node quadrilaterals) and found that both the sums of the eigenvalues and the end loading of cantilever beam models show the composite elements to be significantly softer than the corresponding isoparametric elements. No comment is made concerning the amount of improvement corresponding to the various types of strain.

In addition, it was observed in this study that the composite quadrilateral elements using the scale-free formulation required approximately one-quarter the execution time to generate than the commonly used isoparametric quadrilateral element that is integrated numerically using the Gauss quadrature method. This result came from timing the execution of the respective subroutines formulating the stiffness matrices. There is no compilation time or other

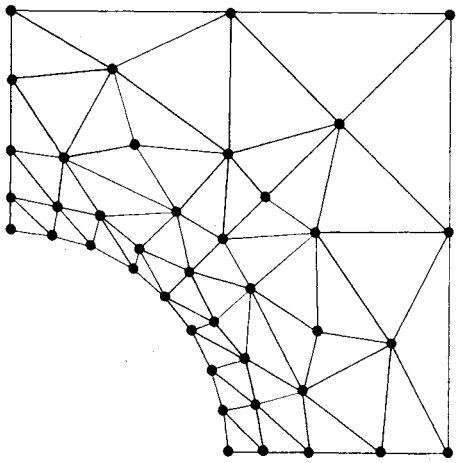

Fig. 8 Fine mesh quarter-section with 58 elements.

operations involved in this comparison. These tests were run on a Control Data 6400 using version 5.4 of the University of Minnesota Fortran compiler.

The analysis of the eigenvalues of distorted quadrilateral elements leads to the conclusion that composite elements utilizing scale-free constant-strain triangles are more accurate than isoparametric elements. This is substantiated by comparing the tip deflections of end-loaded cantilever beams modeled with the two types of elements. In addition, the composite elements require approximately one-quarter the execution time to compute than the isoparametric elements. Isoparametric elements are better at representing square and rectangular elements, but recursively generated square elements and hence, recursively generated rectangular elements are more accurate than the isoparametric elements. The stiffness properties of these composite elements are unchanged when they are generated at an arbitrary rotation and displacement. Thus, the stiffness properties are invariant with respect to orientation and location. It is concluded that constant strain triangles are preferable to isoparametric elements in cases where distorted shapes are required.

Stress Concentration Application

Complex stress concentration problems can be modeled using large numbers of scale-free and dimensionless elements with good accuracy and without introducing a large number of degrees of freedom or numerical difficulties into the overall problem. The resulting refined stiffness matrix formulated using numerical calculations instead of analytic manipulations using symbols is dimensionless. The dimensionless feature results in a stiffness matrix that is applicable to problems of different physical dimension. Thus, the procedure of using scale-free and dimensionless elements with static condensation procedures is an extension and a generalization of the refined-element method. A stress concentration problem is illustrated with the case of a square shear panel containing an internal circular hole that has a diameter of one-half the edge length of the square. The stress concentration element is analyzed as a separate structure and as a component of a larger structure to determine its convergence and stiffness properties.

The convergence of the strain energy for identical stress concentration elements with different degrees of mesh refinement is studied using eigenvalue techniques. The coarse mesh has 64 elements and 96 degrees of freedom and the fine mesh has 232 elements and 280 degrees of freedom. Since the problem is symmetric, the overall stiffness matrix is assembled from quarter sections of the panel and the internal degrees of freedom are eliminated as is convenient. The fine mesh configuration for a quarter-section is shown in Fig. 8. The final stiffness matrix in both cases contains only 32

Table 7 Strain energy for distinctive modes and sum of all modes for both coarse and fine meshes

Mode type	Strain energy (0.5×10^8) Coarse mesh	Fine mesh
Shear	0.03128	0.02746
Pinching	0.03817	0.02664
Pinching	0.05630	0.05346
Extension	0.08602	0.08275
Flexure	0.19176	0.11261
Extension	0.20373	0.18181
Shear	0.22959	0.20517
Flexure	0.24839	0.24145
Shear	0.27467	0.23586
Pinching	0.29740	0.25186
Extension	0.30197	0.26381
Extension	0.43565	0.33529
Pinching	0.50043	0.24058
Shear	0.50304	0.34938
Flexure	0.55211	0.28913
Sum of all strain energy	7.89132	5.78480

Table 8 Stress concentration factors obtained from analyses refined elements compared to theoretical results

Diameters from edge	Analysis using refined element	Theoretical results (10)	Refined to theoretical, %
	Stress concentration located at upper side of hole		
8.0	2.493	3.00	83
9.5	2.522	3.05	83
11.0	2.525	3.07	82
12.5	2.531	3.10	82
14.0	2.535	3.20	79
15.0	2.866	3.70	78
	Stress concentration located at lower side of hole		
8.0	2.493	3.00	83
9.5	2.520	3.04	83
11.0	2.522	3.05	83
12.5	2.526	3.07	82
14.0	2.532	3.09	82
15.0	2.680	3.20	84

degrees of freedom. These coordinates are the edge nodes used to interface the meshes of the stress concentration element and the rest of the structure and are the only coordinates directly introduced into the overall problem. If the hole is to be loaded internally, additional degrees of freedom would be needed to accommodate these applied loads. The stress distribution is determined with auxiliary calculations using a stress transformation matrix that is a linear function of the dimensions of the problem.

The eigenvalues and eigenvectors of the coarse mesh element are computed and the 32 linearly independent eigenvectors are then used to determine the strain energy contained in both stress concentration elements. Four shear modes, four pinching modes, four pure extension modes, and three flexure modes are identified when the eigenvectors are studied. The strain energy corresponding to these modes and the total strain energy for the sum of the 29 flexible modes are given in Table 7. The strain energy for each mode is smaller for the fine mesh than for the coarse mesh. This is also the case for each of the 14 modes not specifically shown in the table. Thus, the fine mesh element is a better model of the problem than the coarse mesh element.

The coarse mesh stress concentration element is used as part of a larger structure to illustrate the use of the element. The element is used to model a hole at various positions in a square with a 16 diam edge length and loaded with a uniaxial tension. The resulting stress concentration factors at two locations around the hole are compared with theoretical values for a hole at various positions in an infinite strip with an overall width of 16 diameters. The center of the hole is located 8.0, 9.5, 11.0, 12.5, 14.0, and 15.0 diameters from the edge of the strip. The resulting stress concentration factors are compared in Table 8. In each case, the finite-element stress concentration factors on both sides of the hole are less than those for the infinite strip by approximately the same amount. The significance of this result is that the accuracy of the stress concentration factor remains essentially constant when the element is located at different positions in the stress field. The absolute accuracy of the finite-element solution is improved when a finer mesh is utilized. This has been demonstrated for the case of a strip with a width of 16 diameters containing a centered hole modeled using constant strain triangles under several loading conditions, including uniaxial tension.[9]

Conclusion

The developments presented here are recursive techniques and, hence, differ from the majority of work that has gone into improving the finite element method which can be classified as either microscopic or macroscopic developments. The recursive techniques use the finite element method to improve itself. The important microscopic improvements focus on detailed modeling of more complex behavior, material properties, and boundary conditions by using more involved element formulation processes. Examples of such developments are hybrid elements, interface elements, boundary elements, and fracture elements. The equally important macroscopic improvements focus on the development of generalized programs, specialized programs, more efficient solution routines, automatic grid generation methods, etc.

The developments presented here are classified as recursive techniques because scale-free finite elements are used in conjunction with standard finite element assembly and static condensation techniques to produce dimensionless finite elements. Since these dimensionless elements are applicable to problems of different physical dimensions, this procedure can be seen as a generalization on the refined element technique. This generalization is possible since the limitation on the refined element method due to the magnitude of the effort to perform the required calculations has been eliminated through the use of numerical calculations.

Dimensionless stress concentration elements can be developed without special software by using almost any standard finite element program equipped with a constant strain triangle element. In fact, a four-node isoparametric element reduced to a triangle by locating two nodes at the same point results in a constant strain triangle and can be used to formulate these dimensionless elements. However, the use of the general dimensionless triangular element shown here would reduce the required computer time.

Since these elements are applicable to problems of different physical dimensions, one can envision dictionaries of dimensionless stress concentration elements that have been thoroughly tested against theoretical results and other finite element solutions. The use of these dictionary elements would reduce the effort required by the analyst because the precalculated stress concentration elements would be available from a tape or a disk file. Confidence in the results of analyses would increase because the dictionary elements would be extensively tested. This testing, which the individual analyst usually does not have the time or resources to perform, is economically justified since the stress concentration element is dimensionless and can be applied to problems of different physical dimensions. It is anticipated that similar procedures can be applied to three-dimensional problems.

Acknowledgments

Support under National Science Foundation Grant PFR-7823078 to the University of Colorado is gratefully acknowledged. The authors also thank the Earth Dams Section of the Division of Design of the Water and Power Resources Service (formerly the Bureau of Reclamation) for its assistance.

References

[1] Cook, R. D., *Concepts and Applications of Finite Element Analysis*, John Wiley and Sons, Inc., New York, 1974.

[2] Desai, C. S. and Abel, J. F., *Introduction to the Finite Element Method*, Van Nostrand Reinhold Co., New York, 1972.

[3] Fried, I., "Accuracy of Complex Finite Elements," *AIAA Journal*, Vol. 10, March 1972, pp. 347-349.

[4] Henshell, R. D., Walters, D., and Warburton, G. B., "A New Family of Curvilinear Elements for Vibration and Stability," *Journal of Sound and Vibration*, Vol. 20, Feb. 1972, pp. 381-397.

[5] Fried, I., "Possible Loss of Accuracy in Curved (Isoparametric) Finite Elements—Comment on a Paper by Henshell, Walters and Warburton," *Journal of Sound and Vibration*, Vol. 23, Aug. 1972, pp. 507-510.

[6] Henshell, R. D., Walters, D., and Warburton, G. B., "On Possible Loss of Accuracy in Curved Finite Elements," *Journal of Sound and Vibration*, Vol. 23, Aug. 1972, pp. 510-513.

[7] Thomas, K., "Effects of Geometric Distortion on the Accuracy of Plane Quadratic Isoparametric Finite Elements," ASCE Meeting Preprint 2504, 1974, pp. 161-203.

[8] Stricklin, J. A., Ho, W. S., Richardson, E. Q., and Haisler, W. E., "On Isoparametric vs. Linear Strain Triangular Elements," *International Journal for Numerical Methods in Engineering*, Vol. 11, No. 6, 1977, pp. 1041-1043.

[9] Radaj, D., "Accuracy of the Finite Element Analysis for the Elastic Plate with a Circular Hole," *International Journal for Numerical Methods in Engineering*, Vol. 6, No. 3, 1973, pp. 443-447.

[10] Peterson, R. E., *Stress Concentration Factors*, John Wiley and Sons, Inc., New York, 1974.